

Sub-Femtomole Peptide Detection in Ion Mobility-Time-of-Flight Mass Spectrometry Measurements

John A. McLean and David H. Russell*

The Laboratory for Biological Mass Spectrometry, Department of Chemistry, Texas A&M University, College Station, Texas 77843

Received January 22, 2003

Abstract: Sensitivity and detection limit enhancements are obtained for peptides by performing high repetition rate (150 Hz) matrix-assisted laser desorption/ionization (MALDI) coupled with ion mobility-time-of-flight mass spectrometry. Absolute limits of detection (3σ) for model peptides are on the order of 0.1 fmol of peptide deposited and represent a factor of 40–60 improvement over data obtained using typical low repetition (20 Hz) MALDI. This increase in sensitivity is demonstrated for two-dimensional MALDI-IM-TOFMS peptide mass mapping of bovine hemoglobin.

Keywords: ion mobility • time-of-flight mass spectrometry • matrix-assisted laser desorption/ionization • high repetition rate • two-dimensional separation • peptide mass mapping

Introduction

The two-dimensional gas-phase separation of biologically important molecules by ion mobility (IM) time-of-flight mass spectrometry (TOFMS) provides several unique advantages over mass spectrometry alone. Because IM provides a separation mechanism proportional to the collision-cross-section of the molecule, in some cases IM can be used to resolve structural isomers,¹ or conformations of peptides² and proteins,³ prior to mass analysis. Such measurements have significant utility for proteomics, i.e., applications to studies of secondary/tertiary structure⁴ and screening for post-translational modifications.⁵ Further, molecules of different classes (e.g., oligonucleotides, peptides, lipids, etc.) are readily separated owing to general conformational motifs that these molecules adopt in the gas phase.⁶ In the analysis of complex biological samples, this provides three primary benefits: (i) qualitative identification of the molecular class(es) present, (ii) suppression of chemical noise, and (iii) the potential for high mass measurement accuracy by using internal calibrants that do not interfere with the analyte of interest.⁶ However, the fundamental challenge in developing IM-TOFMS instrumentation for addressing proteomic-scale questions is that the IM-TOFMS technique typically suffers from poor sensitivity and limits of detection (nmol–pmol). This is attributed to several factors including poor ionization efficiency, poor ion transmission efficiency from the point of ion production to the ion mobility drift cell,

ion loss in the uniform electrostatic-field drift cell (by diffusion and scattering processes), and ion losses that arise due to poorly imaging the ions emanating from the ion source onto the differential aperture used to separate the drift cell from the high vacuum mass spectrometer.

Several directions have been pursued by a number of groups to address these fundamental sensitivity issues. For example, advances in pulsed ion funnels⁷ and pulsed ion traps⁸ as ion transmission and storage devices can significantly improve sensitivity when coupling a continuous ion source such as electrospray ionization (ESI) with IM-MS. Periodic-focusing nonuniform electrostatic-field drift cells can further increase ion transmission efficiency by factors of ~ 10 – 1000 over comparable uniform electrostatic-field designs without a concomitant degradation in ion mobility resolving power.⁹ Indeed, by using a ~ 30 -cm periodic-focusing drift cell a signal-to-noise (S/N) ratio of ~ 10 was obtained for 6 fmol of the peptide α -MSH (Ac-SYSMEHFRWGKPV, MW = 1665.78 Da) using matrix-assisted laser desorption/ionization (MALDI) IM-TOFMS at a laser repetition rate of 20 Hz.⁹ Although MALDI and ESI are both effective for producing biomolecular ions for IM-MS,^{10,11} owing to their differences in terms of the types of ions formed and ionization efficiency the source selected will depend on the aim of the experiment. To address the high-throughput and high-sensitivity demands of proteomic-scale studies, MALDI is well suited because it produces predominantly singly charged ions; thus, the analyte ions are contained in a single signal rather than being partitioned into several charge states. Further, MALDI produces ions in both a temporally focused plane (ns–ps) and a spatially focused region (μm^2) of dimensions similar to the differential aperture (200–350 μm diameter) at the terminating end of the ion mobility drift cell. Consequently, ion mobility drift time resolution is not limited by temporally gating the injection of ions into the drift cell as required by continuous ion sources such as ESI.¹² This becomes increasingly important when operating at higher field strengths and subsequently faster drift times. However, the primary limitations of MALDI stem from the low repetition rate lasers that are commonly used (e.g., cartridge-type N_2 lasers, 10–30 Hz). It is performing MALDI at low repetition rates that ultimately limits the duty cycle and consequently the sensitivity in typical MALDI-TOFMS experiments. For example, at 20 Hz, ions are injected into the IM-TOFMS every 50 ms. If we assume an arrival time distribution for the ion mobility dimension of 2 ms, the instrument duty cycle is limited to 4%. By operating at MALDI repetition rates of 150 and 500 Hz, the

* To whom correspondence should be addressed. Tel: 979-845-3345. Fax: 979-845-9485. E-mail: russell@mail.chem.tamu.edu.

instrument duty cycle is improved to 30 and 100%, respectively. Recently, moderate energy (10–30 $\mu\text{J}/\text{pulse}$) high-repetition rate (up to kHz), solid-state, frequency-tripled (355 nm) Nd:YAG lasers have become available. Indeed, atmospheric pressure MALDI-quadrupole-TOFMS experiments performed at 1 kHz with a Nd:YAG laser provided up to a factor of 80 enhancement in sensitivity in comparison with results obtained using a N_2 laser at 30 Hz.¹³ In these studies, the utility of performing high repetition rate MALDI-IM-TOFMS was demonstrated for the analysis of several model peptides and for a tryptic digest of hemoglobin.

Experimental Section

MALDI-IM-TOFMS at High and Low Repetition Rates.

Briefly, the IM-TOFMS instrument consists of a 31-cm long periodic-focusing drift cell⁹ followed by an orthogonal two-stage reflectron TOFMS (60-cm flight path). MALDI was performed by using a frequency-tripled microcrystal Nd:YAG laser (Model PowerChip PNV, JDS Uniphase), which was externally triggered at variable repetition rates (50–500 Hz). In these experiments, the total drift time acquisition was 2 ms, which yields a maximal MALDI repetition rate of 500 Hz to preserve drift time- m/z correlation. Although data acquisition at MALDI repetition rates > 150 Hz exceeds the time-to-digital converter (TDC) list-mode readout rate of the current instrument, state-of-the-art TDC technology will allow operation at much higher MALDI repetition rates (1–5 kHz).¹⁴ For comparison purposes, results were obtained by using a nitrogen laser (Model VSL-337ND-S, Spectra-Physics, Thermo Laser Science Products, Mountain View, CA) at 20 Hz repetition rate.

Samples and Preparation. The peptides and protein used in these studies, human angiotensin I (American Peptide Co., Inc., Sunnyvale CA), human angiotensin II (American Peptide Co.), and bovine hemoglobin (Sigma-Aldrich, St. Louis, MO), were used without further purification. Enzymatic digestion of hemoglobin was performed by using sequencing grade modified trypsin (Promega, Madison, WI) with thermal denaturation as described elsewhere.¹⁵ Briefly, protein samples were dissolved in 50 mM ammonium bicarbonate (Sigma) and thermally denatured at 90 °C for 20 min. Denaturation was quenched by placing samples in a freezer and followed by trypsin digestion at 37 °C for 4 h. The concentration of trypsin was maintained at 40:1 (weight of substrate/weight of trypsin). For analysis, samples were deposited using the dried droplet technique with α -cyano-4-hydroxycinnamic acid as matrix.

Results and Discussion

Figure 1 illustrates the integrated mass spectral signal intensity obtained using both high and low MALDI repetition rates. In both cases, MALDI was performed until the sample was exhausted (~ 2 min data acquisition). Figure 1A shows the integrated mass spectral signal intensity obtained for 1.2 and 0.96 fmol (deposited) of angiotensin II and angiotensin I, respectively, using a MALDI repetition rate of 150 Hz. Based on a S/N ratio of ~ 30 , this represents a 3σ absolute detection limit on the order of ~ 0.1 fmol of peptide deposited. This detection limit value is further supported by S/N levels obtained for 20 and 200 fmol of peptide deposited. For comparison purposes, Figure 1B illustrates that a S/N of ca. 10 is obtained for 30 fmol angiotensin II and 24 fmol angiotensin I using a nitrogen laser at a repetition rate of 20 Hz. This represents approximately a factor of 40–60 enhancement in the absolute

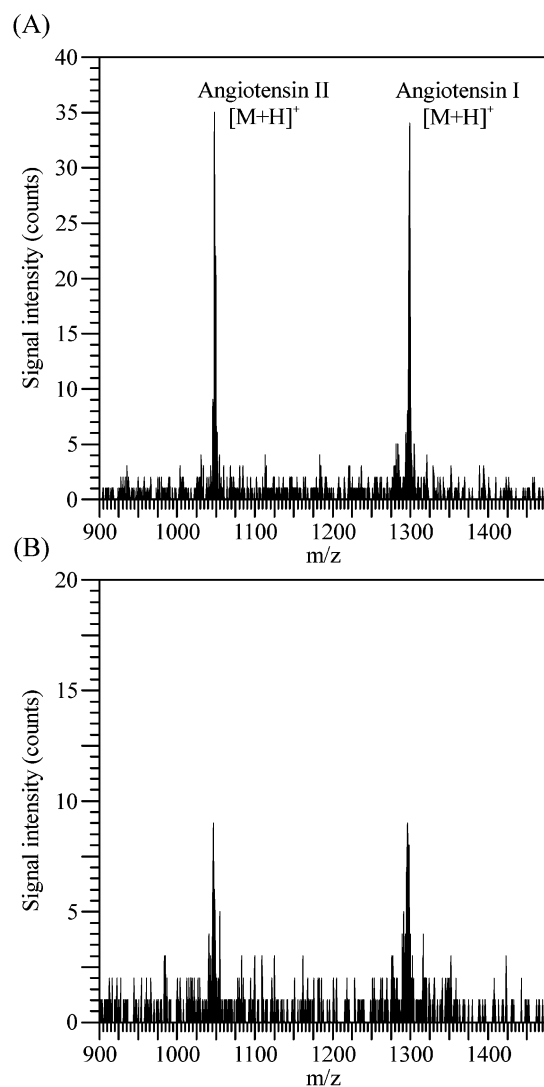


Figure 1. (A) Integrated mass spectrum (over all arrival time distribution space) of a mixture of 1.2 fmol of human angiotensin II (DRVYIHPF, FW = 1045.54 Da) and 0.96 fmol of human angiotensin I (DRVYIHPFHL, FW = 1295.69 Da) deposited on the probe tip. MALDI was performed using a frequency-tripled Nd:YAG laser (355 nm) at a laser repetition rate of 150 Hz. (B) Integrated mass spectrum of a mixture of 30 fmol human angiotensin II and 24 fmol human angiotensin I deposited on the probe tip. MALDI was performed using a nitrogen laser (337 nm) at a laser repetition rate of 20 Hz. In both cases, the drift cell was operated at $62 \text{ V cm}^{-1} \text{ Torr}^{-1}$ with helium gas.

limits of detection by utilizing increased MALDI repetition rates. Alternatively, this enhanced sensitivity can provide a factor of 40–60 increased sample throughput when sample is not limited, where an increase in count rate (counts/s) commensurate with the increase in laser repetition rate is observed.

A typical two-dimensional MALDI-IM-TOFMS peptide mass map for a tryptic digest of bovine hemoglobin (4 pmol (as protein) deposited) is shown in Figure 2. The ion mobility arrival time distribution (Figure 2 (left)) is what would be observed if a detector were placed at the exit aperture of the drift cell, that is, integrating over all m/z space. Similarly, Figure 2 (bottom) is the integrated mass spectrum, which would be obtained in the absence of the ion mobility drift cell. For example, integrating the mass spectrum over drift times of

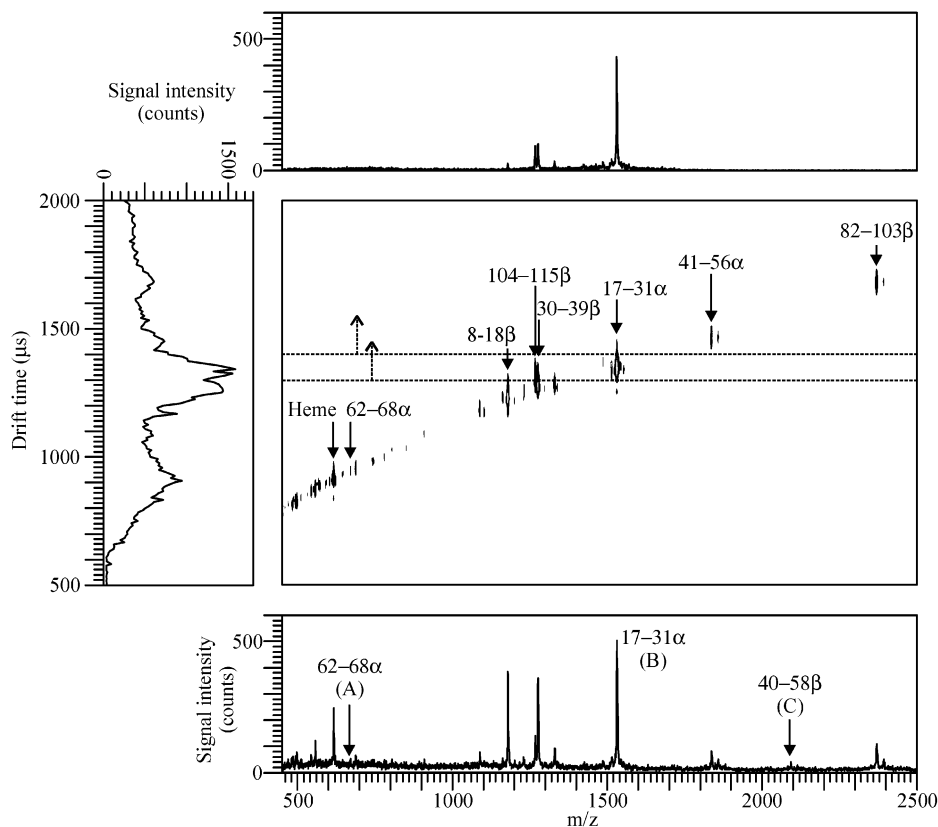


Figure 2. Two-dimensional ion mobility-mass spectrometry map of a tryptic digest of bovine hemoglobin (~4 pmol (as protein) deposited). Several of the most intense peaks are assigned according to their position in the α - or β -chain of the protein, respectively. Left: the arrival time distribution integrated over all m/z space. Bottom: the mass spectrum integrated over all arrival time distribution space. See the text for description of peaks labeled A–C. Top: mass spectrum obtained by integrating over drift times of 1300–1400 μs (region outlined by dashed lines). The drift cell was operated at $80 \text{ V cm}^{-1} \text{ Torr}^{-1}$ with nitrogen gas, and MALDI was performed using α -cyano-4-hydroxycinnamic acid matrix and a frequency-tripled Nd:YAG laser (355 nm) at a laser repetition rate of 100 Hz.

1300–1400 μs provides the mass spectrum as shown in Figure 2 (top). By integrating the mass spectra over this narrow range of drift time (100 μs), the suppression of chemical noise owing to the separation of analytes by ion mobility prior to mass analysis is apparent as elimination of signal outside the selected drift time range and attenuation of background noise in the baseline. The total acquisition time for this two-dimensional peptide mass map was ca. 5 min and was stopped when the most abundant peptide ion peak (17–31 α , VGGHAAEYGA-EALER, $m/z = 1530.64$) reached 500 counts peak height in the integrated mass spectrum. Further, this sample was reanalyzed four times using the same deposited sample. Integrating the total peak counts in the two-dimensional ion mobility-mass spectrometry map yields a dynamic range for peptide ions of ca. 10^2 – 10^3 . For example, the number of integrated counts for peak A (fragment 62–68 α ; VAAALTK, $m/z = 673.83$) and peak C (fragment 40–58 β ; FFESFGDLSTADAVMNNPK, $m/z = 2091.30$) are ~100 and 30, respectively, in comparison with 6050 counts for peak B (fragment 17–31 α). By further signal averaging, this dynamic range should be improved, in particular owing to chemical noise suppression. The pre-separation of peptides by ion mobility prior to mass analysis also reduces ion suppression (e.g., preferential detection of Arg vs Lys terminated tryptic peptide fragments¹⁶) and typically produces higher percent amino acid coverage than MALDI-TOFMS.¹⁷ Although the total amount of sample deposited is higher than that typically used for high vacuum MALDI-TOFMS, this illustrates the data quality

that can be achieved using high repetition rate MALDI on the present instrument.

In addition to the increase in signal intensity afforded by using higher laser repetition rates, the laser spot quality on the sample probe is significantly improved using the Nd:YAG microcrystal laser in comparison with a conventional N_2 laser. For example, the Gaussian-profile of the primary beam of the Nd:YAG laser (~1 mm diameter) can be focused to a spot ~200 μm , whereas the primary beam for the N_2 laser (rectangular ~5 mm \times 7 mm) is focused to an ellipse of ~200 \times 300 μm (as measured on burn paper). Further, the temporal pulse characteristics of the two lasers ~0.5 ns and ~4 ns for the Nd:YAG and N_2 lasers, respectively, favors more efficient MALDI ion yields at shorter pulse widths owing to higher laser fluence rather than irradiance (i.e., energy density).¹⁸ The improved laser spot characteristics of the microcrystal Nd:YAG may also enhance sensitivity by more properly imaging the ion source onto the 350 μm dia. differential aperture of the ion mobility drift cell, similar to the requirements of properly imaging the ion source on to the field-free slits in magnetic and electrostatic sector-field MS instruments.¹⁹

Conclusions

To the best of our knowledge, these are the lowest absolute detection limits obtained for peptides using IM-MS (~0.1 fmol deposited). Importantly, these signal enhancements and those that should be obtained at even higher MALDI repetition rates

allow for the emerging MALDI-IM-TOFMS technique to be used in addressing more challenging topics encountered in proteomics where the amount of sample is limited, high throughput is necessary, or in often cases both.

Acknowledgment. We thank Kent J. Gillig and Brandon T. Ruotolo for their assistance and constructive comments. Financial support for this work is provided by grants from the National Science Foundation (MRI-0116685), the U.S. Department of Energy, Division of Chemical Sciences, BES (DE-FG03-95ER14505), and the Texas Advanced Research Program/Advanced Technology Program (No. 010366-0064-2001).

References

- (1) (a) Karasek, F. W.; Kane, D. M. *Anal. Chem.* **1974**, *46*, 780–782. (b) Tou, J. C.; Boggs, G. U. *Anal. Chem.* **1976**, *48*, 1351–1357. (c) Carr, T. W. *J. Chrom. Sci.* **1977**, *15*, 85–88. (d) Hagen, D. F. *Anal. Chem.* **1979**, *51*, 870–874.
- (2) (a) von Helden, G.; Wyttenbach, T.; Bowers, M. T. *Science* **1995**, *267*, 1483–1485. (b) Wyttenbach, T.; von Helden, G.; Bowers, M. T. *J. Am. Chem. Soc.* **1996**, *118*, 8355–8364.
- (3) (a) Clemmer, D. E.; Hudgins, R. R.; Jarrold, M. F. *J. Am. Chem. Soc.* **1995**, *117*, 10141–10142. (b) Shelimov, K. B.; Jarrold, M. F. *J. Am. Chem. Soc.* **1996**, *118*, 10313–10314. (c) Shelimov, K. B.; Clemmer, D. E.; Hudgins, R. R.; Jarrold, M. F. *J. Am. Chem. Soc.* **1997**, *119*, 2240–2248.
- (4) Ruotolo, B. T.; Verbeck, G. F.; Thomson, L. M.; Gillig, K. J.; Russell, D. H. *J. Am. Chem. Soc.* **2002**, *124*, 4214–4215.
- (5) Ruotolo, B. T.; Verbeck, G. F.; Thomson, L. M.; Woods, A. S.; Gillig, K. J.; Russell, D. H. *J. Proteome Res.* **2002**, *1*, 303–306.
- (6) (a) Koomen, J. M.; Ruotolo, B. T.; Gillig, K. J.; McLean, J. A.; Russell, D. H.; Kang, M.; Dunbar, K. R.; Fuhrer, K.; Gonin, M.; Schultz, J. A. *Anal. Bioanal. Chem.* **2002**, *373*, 612–617. (b) Ruotolo, B. T.; Gillig, K. J.; Stone, E. G.; Russell, D. H.; Fuhrer, K.; Gonin, M.; Schultz, J. A. *Int. J. Mass Spectrom.* **2002**, *219*, 253–267.
- (7) Wyttenbach, T.; Kemper, P. R.; Bowers, M. T. *Int. J. Mass Spectrom.* **2001**, *212*, 13–23.
- (8) Hoaglund, C. S.; Valentine, S. J.; Clemmer, D. E. *Anal. Chem.* **1997**, *69*, 4156–4161.
- (9) Gillig, K. J.; Ruotolo, B. T.; Verbeck, G. F.; Stone, E. G.; Russell, D. H. *Rev. Sci. Instrum.* **2003**, submitted.
- (10) (a) von Helden, G.; Wyttenbach, T.; Bowers, M. T. *Int. J. Mass Spectrom. and Ion Proc.* **1995**, *146/147*, 349–364. (b) Gillig, K. J.; Ruotolo, B. T.; Stone, E. G.; Russell, D. H.; Fuhrer, K.; Gonin, M.; Schultz, J. A. *Anal. Chem.* **2000**, *72*, 3965–3971.
- (11) (a) von Helden, G.; Hsu, M.-T.; Kemper, P. R.; Bowers, M. T. *J. Chem. Phys.* **1991**, *95*, 3835–3837. (b) Clemmer, D. E.; Jarrold, M. F. *J. Mass Spectrom.* **1997**, *32*, 577–592.
- (12) (a) Rokushika, S.; Hatano, H.; Baim, M. A.; Hill, H. H., Jr. *Anal. Chem.* **1985**, *57*, 1902–1907. (b) Watts, P.; Wilders, A. *Int. J. Mass Spectrom. and Ion Proc.* **1992**, *112*, 179–190. (c) Siems, W. F.; Wu, C.; Tarver, E. E.; Hill, H. H., Jr.; Larsen, P. R.; McMinn, D. G. *Anal. Chem.* **1994**, *66*, 4195–4201.
- (13) McLean, J. A.; Russell, W. K.; Russell, D. H. *Anal. Chem.* **2003**, *75*, 648–654.
- (14) Fuhrer, K.; Gonin, M.; McCully, M. I.; Egan, T.; Ulrich, S. R.; Vaughn, V. W.; Burton, W. D., Jr.; Schultz, J. A.; Gillig, K. J.; Russell, D. H. Monitoring of Fast Processes by TOFMS. In *Proceedings of the 49th ASMS Conference on Mass Spectrometry and Allied Topics*; Chicago, IL, May 2001; American Society for Mass Spectrometry: Santa Fe, NM, 2001.
- (15) (a) Park, Z.-Y.; Russell, D. H. *Anal. Chem.* **2000**, *72*, 2667–2670. (b) Russell, W. K.; Park, Z.-Y.; Russell, D. H. *Anal. Chem.* **2001**, *73*, 2682–2685.
- (16) Krause, E.; Wenschuh, H.; Jungblut, P. R. *Anal. Chem.* **1999**, *71*, 4160–4165.
- (17) (a) Ruotolo, B. T.; Gillig, K. J.; Stone, E. G.; Russell, D. H.; Fuhrer, K.; Gonin, M.; Schultz, J. A. *Int. J. Mass Spectrom.* **2002**, *219*, 253–267. (b) McLean, J. A.; Ruotolo, B. T.; Gillig, K. J.; Russell, D. H. Enhanced Protein Coverage in Peptide Mass Mapping with MALDI-Ion Mobility-TOFMS Using Different Drift Gases, *2002 Lost Pines Molecular Biology Conference*; Smithville, TX, Oct 2002.
- (18) Beavis, R. C. *Org. Mass Spectrom.* **1992**, *27*, 864–868.
- (19) Berry, C. E. *Rev. Sci. Instrum.* **1956**, *27*, 849–853.

PR034004P